Accepted Manuscript

High performance aligned short natural fibre - epoxy composites

K.L. Pickering, Tan Minh Le

PII: S1359-8368(15)00590-9

DOI: 10.1016/j.compositesb.2015.09.046

Reference: JCOMB 3813

To appear in: *Composites Part B*

Received Date: 20 August 2015

Revised Date: 22 September 2015

Accepted Date: 24 September 2015

Please cite this article as: Pickering KL, Le TM, High performance aligned short natural fibre - epoxy composites, *Composites Part B* (2015), doi: 10.1016/j.compositesb.2015.09.046.

High performance aligned short natural fibre - epoxy composites

K.L. Pickering [a] and Tan Minh Le [a, b*]

[a] School of Engineering, The University of Waikato, Gate 8, Hillcrest Road, Hamilton, 3116, New Zealand

[b] Department of Textile Technology, Hanoi University of Science and Technology, Dai Co Viet Street, Hanoi, Vietnam

* Corresponding author
Phone: +84438681997
Fax: +84438692401
Email: tan.leminh@hust.edu.vn

Abstract

Aligned short harakeke fibre (New Zealand flax) mats were produced using dynamic sheet forming, impregnated with epoxy resin, then pressed and cured on a compression moulder to manufacture composite materials. These composites were found to have significantly higher tensile properties than planar random oriented short fibre composites; the tensile strength (136 MPa) obtained for the composites is higher than any seen in the literature to date for short natural fibre composites. Fibre orientation was not affected by fibre content despite the higher processing pressure required and fibre orientation factors obtained from Modified Rule of Mixtures equations for Young's modulus and tensile strength were found to be similar.

Keywords: A. Polymer-matrix composites (PMCs); B. Mechanical properties; D. Mechanical testing; E. Compression moulding.

1. Introduction

Fibre orientation is an important parameter that affects the mechanical properties of composites including natural short fibre reinforced composites. Even basic models for composite strength support that alignment is a major factor determining mechanical properties, through the use of an orientation factor, including the following Modified Rule of Mixtures for composite strength [1]:

$$\sigma_c = k_1 k_2 \sigma_f V_f + \sigma_m (1-V_f) \quad (1)$$

where k_1 is an orientation factor; σ and V are average tensile strength and volume fraction, respectively; subscripts c, f and m denotes composite, fibre and matrix, respectively; k_2 is the length efficiency factor (incorporating to interfacial strength).

Reinforcing fibres aligned parallel to the direction of the applied load provide the greatest composite strength. Long natural fibre can be easily aligned by hand combing [2, 3] or hand carding machines [4, 5]. Alternatively, intermediate processing can also be conducted such as that carried out for textile fibre including spinning to produce continuous material that can then be directionally controlled during composite manufacture, although this requires substantial infrastructure. It is more difficult to control alignment of short fibres, however, some degree of alignment can occur in processes involving material flow such as extrusion and injection moulding, although fibre can also be damaged during such processes. Production of aligned short natural fibre mats that could be used in compression moulding with both thermoplastic and thermosetting matrices to make composites sets a challenge.

In this work, dynamic sheet forming, a technique normally used to make paper sheets, was used to prepare aligned short harakeke mats. Tensile properties of epoxy matrix composites made from these mats using compression moulding were evaluated and compared with randomly oriented short harakeke fibre-epoxy composites. Orientation of fibres in composites was also quantitatively estimated.

2. Experimental

2.1 Materials

Long fibre bundles extracted mechanically from leaves of harakeke plants were obtained from the Templeton Flax Mill, Riverton, New Zealand and then were alkali treated at elevated temperatures for pulp which would be used as reinforcement in this work. The matrix was a low viscosity epoxy system comprised of Nuplex resin R180 and Nuplex standard hardener H180 (mixing ratio 5:1 by weight).

2.2 Methods

2.2.1 Fibre pulping

Harakeke fibre bundles were initially granulated using a mesh with holes diameter of 4 mm and then pulped using a laboratory scale pulp digester to remove unwanted fibre components and to break down fibre bundles into finer bundles and even single fibres (individual cells). Pulping conditions were similar to those published previously for harakeke fibre [6, 7]; fibre (70 g) and 2% NaOH solution with ratio of 1: 8 by weight were placed in a stainless steel canister. Canisters were then heated in a digester with a set programme so that the temperature was elevated from ambient to 170^{o}C over 90 min and then held for 40 min. The pulp was cooled and thoroughly washed with water, then dried in an oven at 80^{o}C for 24 hours. A pulp yield of 51% was determined from the weight of oven-dried pulp and raw fibre. Dried pulp was stored in air tight bags for later use.

2.2.2 Fibre characterisation

Fibre length and diameter were measured using Kajaani Fibrelab electronic sequential fibre analyser. Two samples of approximately 6000 fibres were analysed and a mean fibre length, diameter and fibre length distribution were reported. A few long and (or) coarse fibres which could block the analyser were removed from the sample using tweezers so actual fibre length and diameter could be slightly higher than from those analysed, however, due to the huge number of fibres measured, the difference was assumed negligible.
Density of pulped harakeke fibre was measured based on ASTM D3800-99 which was described in the previous report [8]. Five rolls of pulped harakeke fibre mats weighing about 1 g were oven dried at 60^{o} C for 72 hours and then placed in a vacuum oven at room temperature for 5 minutes to remove trapped air between fibre cells before testing. An average density was obtained.

Thirty single pulped harakeke fibres were tensile tested based on ASTM C 1557-03. The method was described in detail in a previous research [8] with a system compliance value of 0.3136 was applied to obtain Young's modulus of fibres. Average fibre tensile strength and Young's modulus were calculated.

2.2.3 Preparation of fibre mats

Aligned harakeke pulped fibre mats were produced using an automatic dynamic sheet former (DSF) manufactured by Canpa, Canada. The main parts of the machine include a rotating centrifugal drum with screening fabric (called wire) on the inside surface of the drum and a travelling nozzle (Fig. 1). Water is introduced through the nozzle to build up a water wall on the wire which functions as a fibre cushion. The thickness of the water wall can be set depending on the amount of fibre desired. During operation, the traversing nozzle sprays a flow of water and fibres (called stock) onto the wire to build up a fibre layer until the required thickness is obtained. Then the water is removed and a wet fibre web is formed on the wire. In this work, 40g of pulped harakeke fibre diluted in 20 litre of water was prepared to make a fibre web. The web was oven-dried at 80^{o}C for 24 hours and then cut into fibre mats (Fig. 2) with a size of 22 x 15 cm to fit in a compression mould. Planar random oriented harakeke pulped fibre mats were formed by hand. For this, a suspension of fibre in water was poured onto a screen with very fine holes such that fibres were deposited on the screen surface to form a wet fibre mat whilst the water ran through the screen. The mat was press-dried with paper towels and then removed and oven-dried at 80^{o}C for 24 hours. Dried fibre mats were cut to a size of 15 x 15 cm. A fibre mat weight of 105 g/m^2 was determined. Mats were stored in sealed bags for use later.

2.2.4 Fibre mat tensile testing

The tensile testing of fibre mats was based on the Tappi standard T 404 cm-92. Ten strips of 15 x 2 cm for each direction, longitudinal and transverse, were cut from fibre mats and conditioned at 23^{o} ± 3^{o} C and 50% ± 5% relative humidity for at least 40 hours. Strips were then tensile tested using Instron-4204 universal testing machine fitted with a 10 N load cell at a crosshead speed of 1 mm/min. Breaking load was recorded and tensile strength was calculated by dividing the breaking load by the width of the tested specimen. Average longitudinal tensile strength (LTS) and transverse tensile strength (TTS) of ten specimens were reported. The fraction of TTS/LTS varies from 0 to 1, indicating the degree of fibre orientation in the paper, such that when fibres in the paper are randomly oriented, TTS/LTS equals 1; conversely, when fibres are unidirectionally oriented, the ratio is close to 0.

2.2.5 Composite fabrication

Aligned or randomly oriented short fibre mats reinforced epoxy composites were manufactured using compression moulding. Processes of resin impregnation, curing and post-curing were was described previously [8]. Compression pressures of 0.5, 2.0, 3.7, 7.0 and 9.0 MPa were used for fibre contents 12, 27, 33, 46 and 52 wt%, respectively.

2.2.6 Composite evaluation

The density measurement of composites was based on ASTM 792-00. Distilled water was used as an immersion fluid. Densities of five composite specimens were measured and the average density was obtained.

Composite tensile testing was based on ASTM D 3039 which was described in detail in the previous work [8]. Five rectangular specimens with nominal dimensions of 150 x 15 x 3 mm was tested on an Instron-4204 universal testing machine fitted with a 50 kN load cell at a crosshead speed of 5 mm/min. Mean values of tensile strength and Young's modulus of composites were reported.

2.2.7 Microscopy

Fibre surfaces and tensile fracture surfaces of composites were investigated using a Hitachi S4100 field emission scanning electron microscope (FESEM) operated at 5 kV. All samples were mounted on aluminium stubs using carbon tape and then sputter coated with platinum to make them conductive prior to observation.

3. Results and discussion

3.1 Fibre morphology

The SEM image (Fig. 2) shows that not all fibres were separated into single fibres and there were some fibre bundles remaining due to the low concentration of NaOH solution used for fibre pulping. Closer observation (Fig. 3) showed wrinkled fibre surfaces which might enhance the fibre-matrix bonding supporting removal of non-cellulose such as wax, pectin and lignin to reveal surface substructure of the fibre [9]. Fig. 3a shows kink banks [10], naturally occurring fibre defects marked by arrows. However, the number of kink bands observed on pulped harakeke fibres was very small compared to the numbers that have seen in other work on flax fibre [10-13] and hemp fibre [14]. These are believed to be due to the change of microfibril angle relative to the fibre axis at the defect region leading to the change of crystalline orientation [14] and act as a region of weakness in the fibre. At the side of the kink bands, cracks on the surface were observed (Fig. 3b). These defects weaken fibres and could affect the mechanical properties of composites.

3.2 Fibre physical and mechanical properties

The average length and diameter obtained using a Kajaani Fibrelab analyser and density, tensile strength and Young's modulus of pulped harakeke fibres are presented in Table 1. The density of 1.52 g/cm^3 was higher than that of untreated harakeke fibre bundles reported in the previous research (1.27 g/cm^3) [8]. This is likely to be due to non-fibrous materials such as vascular bundles, sheath cells, cuticles and non-cellulose materials such as lignin, pectin and wax being removed during pulping process. Lumen area fraction in harakeke fibre is significant and it should be considered when calculating tensile strength and Young's modulus of fibre [8]. Corrected values for tensile strength and Young's modulus were obtained by dividing measured values by a correcting factor of 0.59 to take account of a lumen area fraction of 41% [8]

3.3 Fibre mat assessment

Fig. 4 shows a fibre mat made using DSF with even fibre distribution and some degree of orientation could be observed. Fibre orientation was further assessed through tensile testing of mats in both longitudinal and transverse directions. The ratio between transverse tensile strength (TTS) and longitudinal tensile strength (LTS) of DSF made mats can vary from 0.1 to 0.9 and as previously mentioned, the lower the TTS/LTS ratio the higher the degree of fibre orientation. A ratio of 0.30 was found in this work indicating good fibre alignment in the fibre mats.

3.4 Evaluation of aligned short fibre composites

The alignment of fibres was also confirmed by SEM micrographs of tensile fracture surfaces of composites (Fig. 5); more fibre ends appear on the images of longitudinal tensile tested sample while more fibre imprints present on transverse tensile one.

Longitudinal tensile properties of composites with fibre contents of 12, 27, 32, 46 and 52 wt% are shown in Fig. 6 and 7 along with transverse and randomly oriented fibre composites with fibre contents of 12 wt% and 46 wt%, respectively. It can be seen that aligned harakeke fibre mats improved tensile strength and Young's modulus of the matrix even at a low fibre content of 12 wt% with increases of 35% and 19%, respectively. Both composite tensile strength and Young's modulus increased with fibre content up to 46 wt%. Further addition of fibres did not improve composite tensile strength or Young's modulus. The longitudinal tensile strength (LTS) of the composites containing 12 wt% fibre was 1.5 times higher than the transverse (TTS) giving a TTS/LTS ratio of 0.69 indicating that fibres were much more aligned on the longitudinal direction, a value higher than that for fibre mat due to the presence of a continuous phase (epoxy resin).

The tensile strength at 46 wt% fibre content of aligned short fibre composite (136 MPa) was 78.5% higher than that of randomly oriented fibre composite (76.2 MPa) and the increase of Young's moduli was 44.6 % (10.5 GPa compared to 7.26 GPa) supporting the improvement brought about by fibre orientation on tensile properties of short fibre composites. The maximum tensile strength and Young's modulus of 136 MPa and 10.5 GPa, respectively at fibre content of 46 wt% for longitudinal tensile tested samples are higher than any reported in the literature to date for natural fibre composites excluding those where hand-layup or a continuous fibre form has been produced and furthermore, these values overlap with those achieved using these procedures. So improved alignment here has more than compensated for the shorter length used, which also gives potential for use with waste fibre. Good bonding between pulped harakeke fibres and the matrix and fewer defects compared to bast fibres which were discussed in Section 3.1 are likely to have contributed to the tensile properties of pulped harakeke fibre-epoxy composites. However, the main reason appears to be due to fibre alignment as discussed above.

3.5 Determining fibre orientation factors

Given that fibre orientation is influential on performance, it is valuable to be able to assess the degree of orientation. Confusion arises in the literature regarding the use of orientation factors. Although different values are found from composite strength and stiffness with their respective modified Rule of Mixtures equations [15, 16], orientation factors used to predict strength and stiffness are sometimes assumed to be the same [17]. In this work, orientation factors are evaluated for strength and stiffness separately.

3.5.1 Fibre orientation factor for Young's modulus.

Young's modulus of aligned short harakeke fibre - epoxy composites taking account of composite porosity can be estimated using the modified Rule of Mixtures:

$$E_c = \eta_o \eta_l E_f V_f + V_m E_m \quad (2)$$

with

$$V_m = 1- V_f - V_p \quad (3)$$

$$V_f = W_f(\rho_c/\rho_f) \quad (4)$$

where ρ, E, W and V are density, Young's modulus, weight fraction and volume fraction, respectively; subscripts c, f, m and p denote composite, fibre, matrix and porosity, respectively; η_o and η_l are orientation efficiency factor and length efficiency factor, respectively. Values from the literature include $\eta_o = 1$ for unidirectional composites, $\eta_o = 0.5$ for bidirectional, balanced ($0/90^o$), $\eta_o = 0.375$ for 2D random and $\eta_o = 0.2$ for 3D random [18, 19].

Porosity of composites was found to be a function of fibre content [8, 20]. In this work, the porosity was modelled as a linear function of fibre volume fraction using linear regression modelling as shown in Fig. 8 :

$$V_p = 0.2031V_f – 0.0028 \quad (5)$$

Substituting Vp from Eq. (5) into Eq. (2), leads to:

$$E_c = \eta_o \eta_l E_f V_f + (1.0028- 1.2031V_f)E_m \quad (6)$$

or

$E_c = (\eta_o\eta_l E_f - 1.2031E_m)V_f + 1.0028E_m$ (7)

The fibre length efficiency factor (η_l) can be calculated using the shear lag model originally developed by Cox [21]:

$\eta_l = 1- \tanh(\beta L/2)/(\beta L/2)$ (8)

where $\beta L/2 = (2L/d)\sqrt{G_m/E_f \ln(\frac{k}{V_f})}$ (9)

where L is fibre length, d is fibre diameter, G_m is shear modulus of matrix, V_f is fibre volume fraction, k is a constant dependant on geometrical packing pattern of fibres [22], equal to 0.907 and 0.785 for hexagonal and square packing respectively.

Assuming k = 0.785, $G_m = E_m/2(1+\nu) = 1.117$ GPa with Poisson's ratio of epoxy $\nu = 0.35$ [23] , Young's modulus of the matrix, $E_m = 3.91$ GPa (Fig. 6), L = 1.97 mm and D =15.67 µm (Table 1), the fibre length factors η_l for different fibre contents were calculated and shown in Table 2.

Using linear regression parameters shown in Fig. 9 and comparing with Eq. (7), it can be seen that

$\eta_o\eta_l E_f - 1.2031E_m = 17.31$ (10)

Substituting $E_f = 47.6$ GPa (Table 1), $E_m = 3.91$ GPa [8] and $\eta_l = 0.99$ (Table 2) into Eq. (10) gives $\eta_o = 0.467$ which corresponds to an average orientation angle $\alpha = 34^o$ considering $\eta_o = \cos^4(\alpha)$ [16, 18].

3.5.2 Fibre orientation factor for tensile strength calculation.

The orientation factor for tensile strength can be estimated using the Bowyer-Bader method [24] that was developed from Kelly-Tyson's [25]. In the Bowyer-Bader model, it can be assumed that at any composite stress there is a critical fibre length (L_ε) such that at the centre of the fibre, the strain of the matrix and fibre are the same and the spectrum of fibre lengths in the composite can be considered to be divided into subcritical subfractions (denoted L_i) and supercritical subfractions (denoted L_j) and their volume fractions are V_i and V_j, respectively. The tensile stress on a composite can be estimated according to Eq. (11).

$\sigma_c = k_1X+k_1Y + Z$ (11)

where X, Y and Z are the contributions of subcritical fibres, supercritical fibre and matrix respectively. They are expanded in following equations:

$X = \sum\frac{\tau L_i V_i}{d}$ with $L_i < L_\varepsilon$ (12)

$Y = \sum E_f\varepsilon_c(1 - E_f\varepsilon_c d/4L_j\,\tau)V_j$ with $L_j > L_\varepsilon$ (13)

$Z = \sigma_m V_m$ (14)

where τ is interfacial shear strength between fibre and matrix; d is fibre diameter; V_m was calculated as in Eq. (3), and

$L_\varepsilon = (E_f \varepsilon_c d)/(2\tau)$ (15)

Values of composite strains at two levels ε_1 and ε_2 are chosen so that $\varepsilon_2 = 2\varepsilon_1$. The composite stresses σ_{c1} and σ_{c2} and matrix stresses σ_{m1} and σ_{m2} corresponding to ε_1 and ε_2 are determined from stress-strain curves of composites and matrix, respectively. With these data, the ratio R can be determined.

$R = (\sigma_{c1} - Z_1)/(\sigma_{c2} - Z_2)$ (16)

To calculate k_1 a value of τ need to be assumed and the corresponding $L_{\varepsilon 1}$ and $L_{\varepsilon 2}$ calculated using Eq.(15). Values of X and Y can then be determined using assumed values of $L_{\varepsilon 1}$, $L_{\varepsilon 2}$ and τ and fibre length distribution. With these assumed values, the ratio R' can be calculated, such that

$R' = (X_1+Y_1)/(X_2+Y_2)$ (17)

The value of τ can then be adjusted until R = R'. This figure can be assumed to be correct and k_1 determined by applying this value to Eq. (11).

The experimental data and fibre length distribution used in the Bowyer-Bader model are presented in Table 3 and Fig. 10, respectively. Orientation factors and IFSS values are reported in Table 4. It can be seen that values of fibre orientation factors for aligned fibre composites at different fibre contents were similar indicating constant orientation despite higher pressure being applied at higher fibre contents. The mean value of orientation factor of 0.505 obtained for aligned fibre composites is significantly higher than that obtained for injection moulded natural fibre composites using the same method of determination [16, 26]. It is also much higher than that for randomly oriented fibre composite (0.312) found in this work which supports that DSF can produce fibre mats with good fibre alignment. The value of orientation factor for tensile strength (0.505) is higher than that for Young's modulus (0.467). However, when comparing their fibre orientation angles, the difference was very small; 33^o for tensile strength and 34^o for Young's modulus, although it is possible that orientation at fracture where strength is assessed is slightly higher than at lower strain where Young's modulus is assessed.

4. Conclusion

Dynamic sheet forming has been shown to be a potential technique to produce aligned short natural fibre mats for composite production using compression moulding. Aligned short harakeke fibre-epoxy composites were produced with this technique with high tensile strength and Young's modulus of 136 MPa and 10.5 GPa, respectively. Fibre orientation factors were also estimated with values of 0.505 and 0.467 relating to average fibre orientation angles of 34° and 33° from values of composite tensile strength and Young's modulus, respectively.

Acknowledgements: The authors would like to thank Vietnamese Government Scholarship Fund for granting a scholarship to T.M Le.

References

[1] Andersons J, Spārniņš E, Joffe R. Stiffness and strength of flax fiber/polymer matrix composites. Polym Compos. 2006;27(2):221-229.

[2] Sawpan MA, Pickering KL, Fernyhough A. Flexural properties of hemp fibre reinforced polylactide and unsaturated polyester composites. Compos Part A. 2012;43(3):519-526.

[3] Newman R, Clauss E, Carpenter J, Thumm A. Epoxy composites reinforced with deacetylated Phormium tenax leaf fibres. Compos Part A. 2007;38(10):2164-2170.

[4] Newman R, Le Guen M, Battley M, Carpenter J. Failure mechanisms in composites reinforced with unidirectional Phormium leaf fibre. Compos Part A. 2010;41(3):353-359

[5] Islam MS, Pickering KL, Foreman NJ. Influence of alkali fiber treatment and fiber processing on the mechanical properties of hemp/epoxy composites. J Appl Polym Sci. 2011;119(6):3696-3707.

[6] Aruan Efendy MG, Pickering KL. Comparison of harakeke with hemp fibre as a potential reinforcement in composites. Compos Part A. 2014;67(0):259-267.

[7] Le Guen MJ, Newman RH. Pulped Phormium tenax leaf fibres as reinforcement for epoxy composites. Compos Part A. 2007;38(10):2109-2115.

[8] Le TM, Pickering KL. The potential of harakeke fibre as reinforcement in polymer matrix composites including modelling of long harakeke fibre composite strength. Compos Part A. 2015;76(0):44-53.

[9] Duchemin B, Staiger M. Treatment of Harakeke fiber for biocomposites. J Appl Polym Sci. 2009;112(5):2710-2715.

[10] Baley C. Influence of kink bands on the tensile strength of flax fibers. J Mater Sci. 2004;39(1):331-334.

[11] Lamy B, Pomel C. Influence of fiber defects on the stiffness properties of flax fibers-epoxy composite materials. J Mater Sci Lett. 2002;21(15):1211-1213.

[12] Baley C. Analysis of the flax fibres tensile behaviour and analysis of the tensile stiffness increase. Compos Part A. 2002;33(7):939-948.

[13] Bos H, Molenveld K, Teunissen W, Van Wingerde A, Van Delft D. Compressive behaviour of unidirectional flax fibre reinforced composites. J Mater Sci. 2004;39(6):2159-2168.

[14] Sawpan MA, Pickering KL, Fernyhough A. Effect of various chemical treatments on the fibre structure and tensile properties of industrial hemp fibres. Compos Part A. 2011;42(8):888-895.

[15] Espinach FX, Julian F, Verdaguer N, Torres L, Pelach MA, Vilaseca F, et al. Analysis of tensile and flexural modulus in hemp strands/polypropylene composites. Compos Part B. 2013;47(0):339-343.

[16] Vallejos ME, Espinach FX, Julián F, Torres L, Vilaseca F, Mutjé P. Micromechanics of hemp strands in polypropylene composites. Compos Sci Technol. 2012;72(10):1209-1213.

[17] Hashemi S. Tensile and flexural properties of injection-moulded short glass fibre and glass bead ABS composites in the presence of weldlines. J Mater Sci. 2008;43(2):721-731.

[18] Krenchel H. In: Fibre reinforcement. Thesis. Alademisk forlag. Copenhagen. 1964.

[19] Madsen B, Thygesen A, Lilholt H. Plant fibre composites–porosity and stiffness. Compos Sci Technol. 2009;69(7):1057-1069.

[20] Madsen B, Lilholt H. Physical and mechanical properties of unidirectional plant fibre composites—an evaluation of the influence of porosity. Compos Sci Technol. 2003;63(9):1265-1272.

[21] Cox H. The elasticity and strength of paper and other fibrous materials. Br J Applied Phys. 1952;3(3):72.

[22] Tucker III CL, Liang E. Stiffness predictions for unidirectional short-fiber composites: review and evaluation. Compos Sci Technol. 1999;59(5):655-671.

[23] Baiardo M, Zini E, Scandola M. Flax fibre–polyester composites. Compos Part A. 2004;35(6):703-710.

[24] Bowyer WH, Bader MG. On the re-inforcement of thermoplastics by imperfectly aligned discontinuous fibres. J Mater Sci. 1972;7(11):1315-1321.

[25] Kelly A, Tyson WR. Tensile properties of fibre-reinforced metals: Copper/tungsten and copper/molybdenum. Journal of the Mechanics and Physics of Solids. 1965;13(6):329-350.

[26] Serrano A, Espinach FX, Julian F, del Rey R, Mendez JA, Mutje P. Estimation of the interfacial shears strength, orientation factor and mean equivalent intrinsic tensile strength in old newspaper fiber/polypropylene composites. Compos Part B. 2013;50(0):232-238.

Table 1: Average physical and mechanical properties of pulped harakeke fibre.

	Length (mm)	Diameter (µ)	Density (g/cm3)	Tensile strength (MPa)	Young's modulus (GPa)	Corrected strength (MPa)	Corected Young's modulus (GPa)
Mean	1.97	15.67	1.52	756	28.1	1281	47.6
SD			0.03	244	15.6	414	26.4

Table 2: Physical properties of pulped harakeke fibre composites.

wt%	W_f	ρ_c (g/cm^3)	V_f	ρ_{ct} (g/cm^3)	V_p	η_l
12.3	0.123	1.175	0.095	1.192	0.015	0.9892
26.7	0.267	1.189	0.209	1.234	0.036	0.9914
33.4	0.334	1.184	0.260	1.252	0.054	0.9922
46.3	0.463	1.22	0.372	1.293	0.056	0.9936
52	0.520	1.182	0.404	1.304	0.094	0.9939

Table 3: Input data for Bowyer-Bader model.

Fibre content wt%	12	27	33	46	52	46 RO*
V_f	0.095	0.209	0.260	0.372	0.404	0.389
ε_1(%)	0.70	0.79	0.80	0.79	0.84	0.71
ε_2.(%)	1.40	1.57	1.61	1.57	1.68	1.42
ε_{max}(%)	2.10	2.36	2.41	2.36	2.52	2.13
σ_{c1}(MPa)	29.3	42.8	45.6	68.0	65.3	64.0
σ_{c2}(MPa)	49.6	69.6	73.7	109.0	103.0	101.0
σ_{cmax}(MPa)	66.20	87.2	100	136	137	76.2
σ_{m2}(MPa)	19.90	21.5	21.5	21.5	21.5	19.2
σ_{m2}(MPa)	36.50	38.8	38.8	38.8	38.8	35.5
σ_{mmax}(MPa)	46.5	47.7	48.0	47.7	48	45.8
E_f(GPa)	47.60	47.60	47.60	47.60	47.60	47.60
d (µm)	15.67	15.67	15.67	15.67	15.67	15.67

* RO = Randomly oriented

Table 4: Fibre orientation factors and interfacial shear strengths.

Fibre content wt%	12	26	33	46	52	46 RO*
Orientation factor k_1	0.505	0.483	0.489	0.531	0.517	0.312
Orientation angle (^{o})	33	34	33	31	32	42
IFSS (MPa)	3.26	3.14	3.17	3.37	3.23	2.47

* RO = Randomly oriented

Fig.1. Centrifugal drum and nozzle of a DSF.

Fig. 2. SEM image of a fibre mat made from pulped harakeke using DSF.

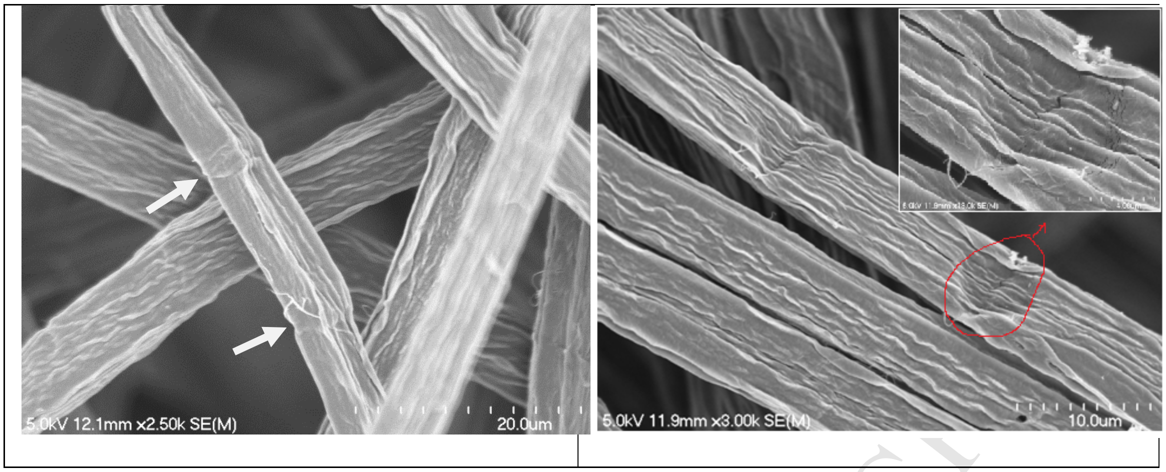

Fig. 3. SEM images of single fibres in a pulped harakeke fibre mat: (a) Single fibres with kink bands marked by arrows and (b) single fibres including an expanded image of a kink band with cracks.

Fig.4. Macrograph of an aligned fibre mat (size of 22 x 15 cm) made from pulped harakeke fibre using DSF.

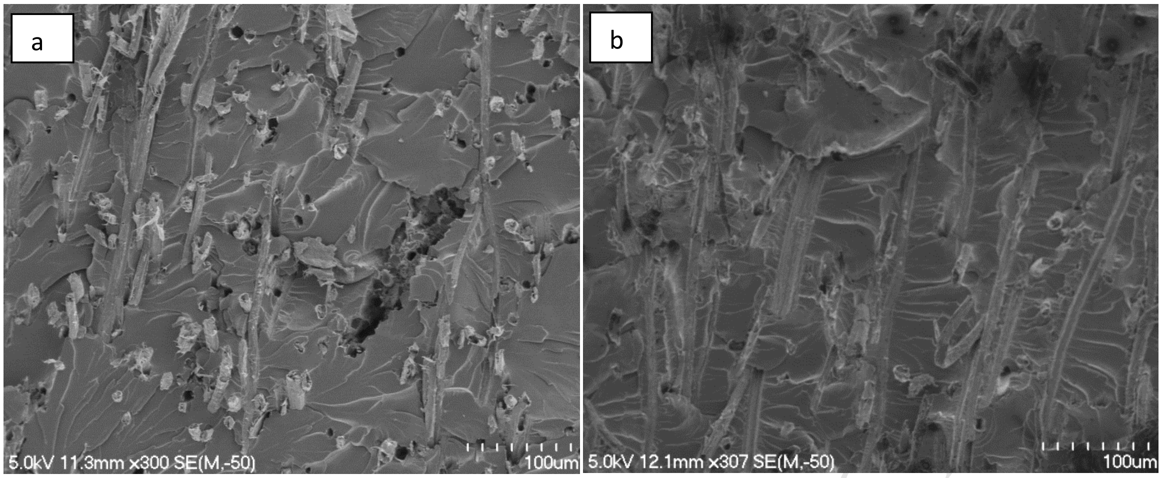

Fig. 5. SEM images of fracture surface of composites: (a) longitudinal tensile sample and (b) transverse tensile sample.

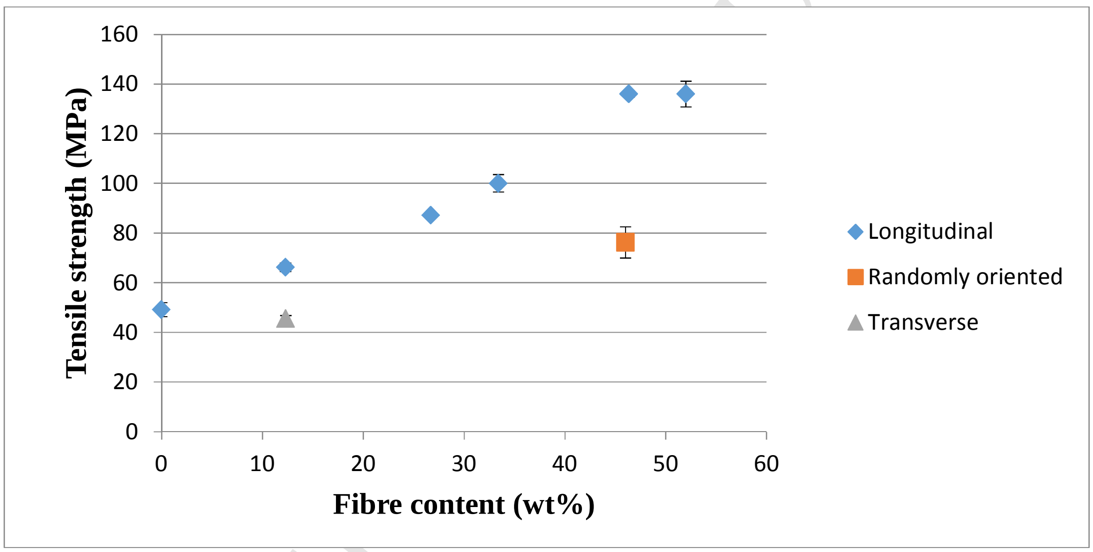

Fig. 6. Tensile strength of pulped harakeke fibre composite as a function of fibre content.

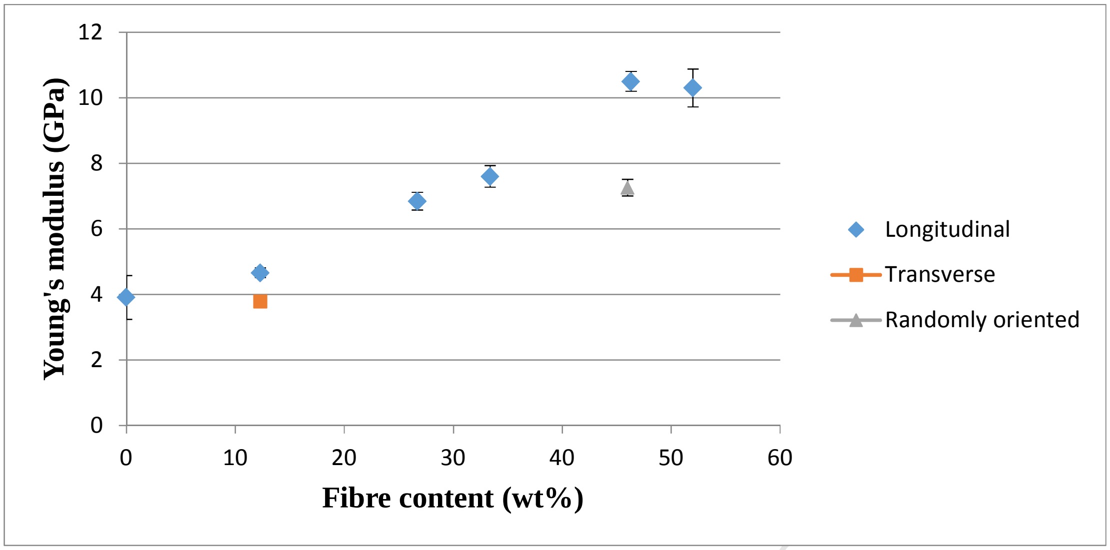

Fig. 7. Young's modulus of pulped harakeke fibre composites as a function of fibre content.

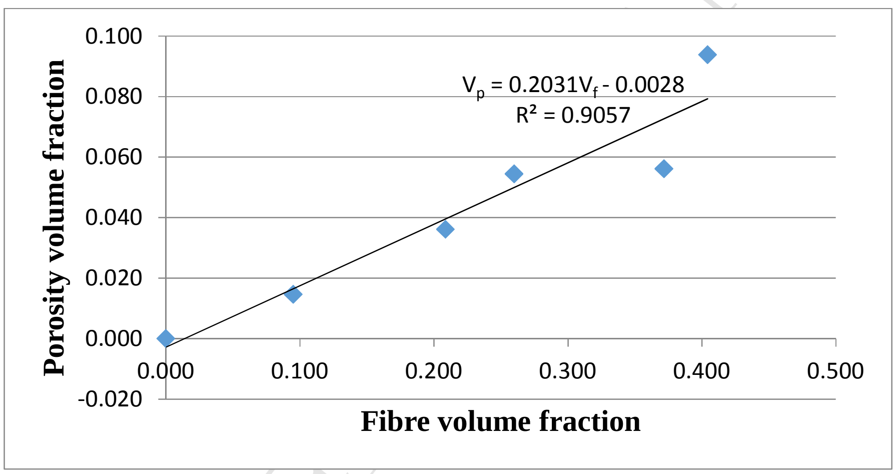

Fig. 8. Porosity as a function of fibre volume fraction.

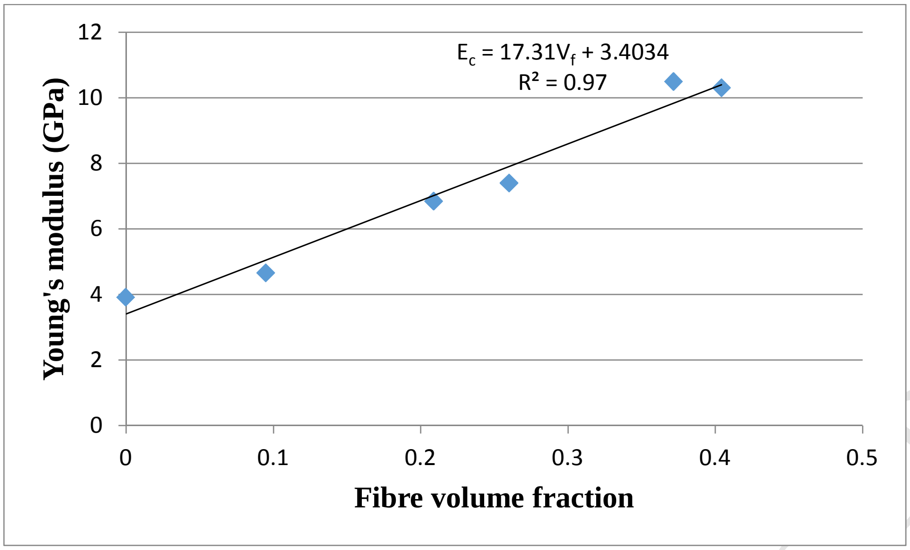

Fig. 9. Young’s modulus as a function of fibre volume fraction including regression equation and R-square value.

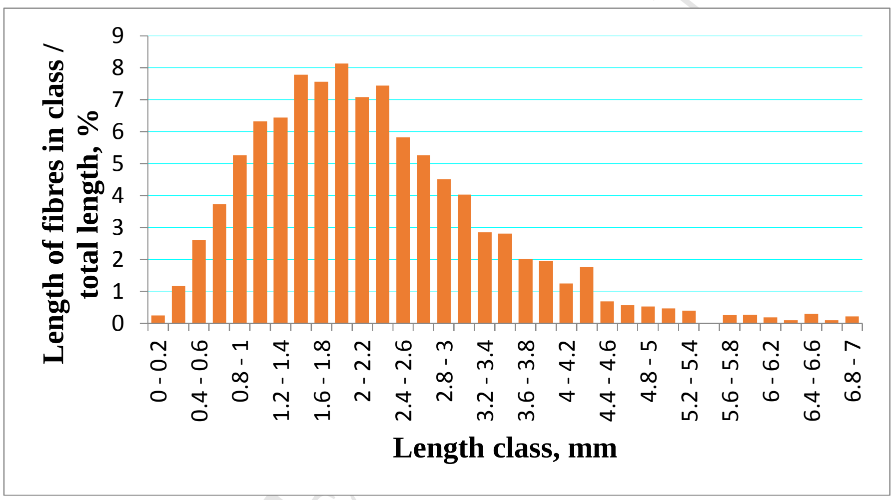

Fig. 10 Fibre length distribution.